



Adsorption of Bisphenol A on KOHactivated tyre pyrolysis char

R. Acosta, D. Nabarlatz, A. Sánchez-Sánchez, J. Jagiello, P. Gadonneix, A.
Celzard, V. Fierro

► To cite this version:

R. Acosta, D. Nabarlatz, A. Sánchez-Sánchez, J. Jagiello, P. Gadonneix, et al.. Adsorption of Bisphenol A on KOHactivated tyre pyrolysis char. *Journal of Environmental Chemical Engineering*, 2018, 6 (1), pp.823-833. 10.1016/j.jece.2018.01.002 . hal-03563505

HAL Id: hal-03563505

<https://hal.univ-lorraine.fr/hal-03563505>

Submitted on 9 Feb 2022

HAL is a multi-disciplinary open access archive for the deposit and dissemination of scientific research documents, whether they are published or not. The documents may come from teaching and research institutions in France or abroad, or from public or private research centers.

L'archive ouverte pluridisciplinaire **HAL**, est destinée au dépôt et à la diffusion de documents scientifiques de niveau recherche, publiés ou non, émanant des établissements d'enseignement et de recherche français ou étrangers, des laboratoires publics ou privés.

Adsorption of Bisphenol A on KOH-activated tyre pyrolysis char

R. Acosta¹, D. Nabarlatz¹, A. Sánchez-Sánchez²,
J. Jagiello³, P. Gadonneix², A. Celzard², V. Fierro^{*2}

¹ INTERFASE, Escuela de Ingeniería Química, Universidad Industrial de Santander. Carrera 27 # 9 Ciudadela Universitaria, Bucaramanga, Colombia. AA674.

² Institut Jean Lamour, UMR CNRS-Université de Lorraine n°7198, ENSTIB, 27 rue Philippe Seguin, BP 21042, 88051 Epinal Cedex 9, France.

³ Micromeritics Instrument Corporation, 4356 Communications Drive, Norcross, GA 30093, United States.

* Corresponding author. Tel: + 33 372 74 96 77. Fax: + 33 372 74 96 38. E-mail address : Vanessa.Fierro@univ-lorraine.fr (V. Fierro)

Abstract

An activated carbon (AC) with a specific surface area of $700 \text{ m}^2 \text{ g}^{-1}$ was prepared by KOH activation of tyre pyrolysis char (TPC) and tested to remove Bisphenol A (BPA) from aqueous solutions. BPA adsorption on this AC was evaluated by studying both the adsorption isotherms at three different temperatures and the decrease of BPA concentration with time, in order to determine the thermodynamic and the kinetic parameters, respectively. The results were compared with those obtained with pristine TPC and with a multipurpose commercial activated carbon (CAC) recommended for BPA adsorption. The present KOH-activated TPC showed a great potential to adsorb BPA with a monolayer capacity as high as 123 mg g^{-1} , higher than that of the CAC used as a reference. BPA adsorption equilibrium data were fitted using different isotherm models with two or three parameters, and the best fitting models were those of Langmuir and Radke-Prausnitz. BPA adsorption was an exothermic process, and the adsorption capacity decreased with increasing temperature. The adsorption kinetics of BPA was adequately described by a pseudo-second order model.

Keywords: Scrap tyre; Porous materials; Bisphenol A, Adsorption capacity; Activated carbon; Adsorption kinetics.

1. Introduction

The distribution and abundance of plastic wastes in the environment has quickly increased all over the world, and their harmful effects arouse a great concern. Not only plastics by themselves represent a considerable source of pollution, but their additives can be even more detrimental to the environment. Among them, Bisphenol A (BPA) is one of the most ubiquitous chemicals worldwide, with approximately 5.5 million metric tons produced in 2011 (Rochester 2013) and over 100 tons released into the atmosphere by yearly production (Vandenberg et al. 2009). BPA is mainly used in the production of polymers, such as polycarbonate, polyacrylate or epoxy resins. This chemical is found in a huge range of products, including eyeglass lenses, CDs and DVDs, personal computers, power tools, sports equipment, medical devices, and food and drink containers. This continuous exposition to BPA has been reported to be a serious cause of human chronic diseases (Rezg et al. 2014). BPA is a chemical intermediate, a monomer, that was first developed as a synthetic oestrogen in the 1890s and reported to stimulate the female reproductive system in rats in the 1930s (Rochester 2013). BPA is catalogued as an endocrine disrupting compound. Besides, it is a recalcitrant water contaminant, with a low biodegradability and a high resistance to chemical degradation. A comprehensive study on the presence and release of BPA and other endocrine disrupting compounds in drinking water was carried out by Casajuana and Lacorte (Casajuana & Lacorte, 2003) who pointed out the need of better monitoring the organic content in drinking water in general. High BPA concentrations have been already observed in wastewater and wastewater sludge ($0.07 \mu\text{g L}^{-1}$ to $1.68 \mu\text{g L}^{-1}$ and $0.104 \mu\text{g g}^{-1}$ to $0.312 \mu\text{g g}^{-1}$, respectively) (Mohapatra et al. 2011).

Due to its ubiquitous nature and estrogenic activity potential, BPA removal has been studied from several perspectives. Adsorption/degradation using metal oxides

(Koduru et al. 2016), biodegradation (Dai et al. 2016; Mita et al. 2015), advanced oxidation (Pachamuthu et al. 2017), osmotic and ultrafiltration membranes (Zhu & Li 2013), amongst others, have been used for BPA removal. However, these methods are not fully successful in BPA removal and have some drawbacks such as formation of toxic degradation by-products, low working concentration ranges, high cost of reagents and raw materials, and the need for further treatment.

The adsorption of organic contaminants by activated carbons (ACs) is one of the most effective and widely used methods for purifying water (Bautista-Toledo et al. 2005). Many different materials have been used for AC production, including biomass (Skodras et al. 2007), coal (Zhao et al. 2011), petrochemical resins (Kan et al. 2016), industrial waste materials like scrap tyres (Mui et al. 2010b) or PET bottle wastes (Mendoza-Carrasco et al. 2016). The application of char and ACs from tyre rubber for wastewater treatment has been reported, including for the sorption of dyes (Mui et al. 2010a), organic pollutants (Alamo-Nole et al. 2011) and heavy metals (Manchón-Vizuite et al. 2005). The sorption efficiency and capacity not only depend on the sorbent structural and chemical properties, but are also strongly influenced by the molecular characteristics of the adsorbates, such as hydrophobicity, polarity and molecular structure (Lian et al. 2013). Several studies reported BPA removal by ACs (Tsai et al. 2006) as well as by sewage sludge (Clara et al. 2004), porous resins (Fan et al. 2011) or carbon nanomaterials, such as graphene, fullerenes and carbon nanotubes (Pan et al. 2008). However, the latter carbon materials are much more expensive than activated tyre pyrolysis char or any other type of activated carbon as stated by the smart review of Sweetman et al. (2017) dealing with the applications of graphene, carbon nanotubes and activated carbons to advanced water purification.

In a previous study, a series of ACs were prepared from rubber tyre pyrolysis char (TPC), and their potential for adsorbing a common antibiotic, tetracycline, was examined (Acosta et al. 2016). Herein, one selected AC produced from TPC was applied to the adsorption of BPA. The present manuscript also comprises a thorough review of BPA adsorption studies carried out so far onto ACs. We demonstrate that tyre-derived ACs are a credible option for BPA adsorption, since capacities as high as 123 mg g⁻¹ were obtained.

2. Experimental

2.1 Adsorbents and reactants

Tyre wastes were pyrolysed to obtain pyrolytic oil with high calorific value. The derived solid residue, here referred to as tyre pyrolysis char (TPC), was used for the production of activated carbons by KOH activation. Tyre pyrolysis as well as activation conditions were extensively reported elsewhere (Acosta et al. 2016; Acosta et al. 2015). Briefly, the only tyre-derived AC used here was prepared at 750°C with a mass impregnation ratio KOH to TPC equal to 5. This carbon was labelled CK.750.5 and was selected because having the highest product $S_{TOT} = S_{BET} \times \text{carbon yield}$ of the ACs series (see section 3.2.2 below). For comparative purpose of the characteristics of the activated carbon produced, a commercial activated carbon (CAC), Hydrodarco C from the company Cabot Norit, was used as reference of offer on the market. Hydrodarco C is indeed a multi-purpose activated carbon, designed to treat industrial wastewaters.

BPA (99% pure; Sigma Aldrich), whose molecular structure is shown in [Figure 1](#), was used to prepare aqueous solutions for adsorption tests.

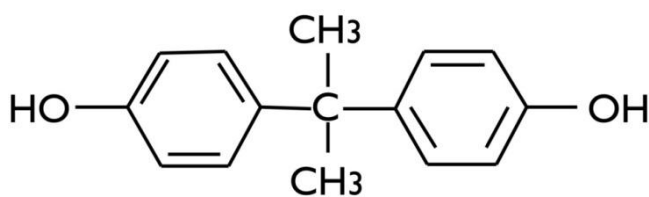


Figure 1. Molecular structure of Bisphenol A (BPA).

2.2 Materials characterisation

An elemental analyser (Vario EL cube, Elementar) was used to determine carbon, hydrogen, nitrogen and sulphur (CHNS) contents of the tested samples. The oxygen content was determined separately with the same apparatus by changing the combustion conditions, and the ash content was determined by difference as described elsewhere (Acosta et al. 2016). The samples were outgassed at 270°C overnight, followed by nitrogen adsorption at -196°C using a 3Flex automatic device (Micromeritics). Micropore volumes, V_{MIC} ($\text{cm}^3 \text{ g}^{-1}$), and micropore surface area were determined by application of the t -plot method, BET surface areas, S_{BET} ($\text{m}^2 \text{ g}^{-1}$), by application of the BET method, and the total pore volumes, V_{TOT} ($\text{cm}^3 \text{ g}^{-1}$), were determined at a relative pressure $P/P_0 = 0.99$ (Gregg & Sing 1982). The mesopore volumes, V_{MES} ($\text{cm}^3 \text{ g}^{-1}$), were determined by difference between V_{TOT} and V_{MIC} (Gregg & Sing 1982). Finally, the points of zero charge, pH_{pzc} (dimensionless) were determined as reported elsewhere (Acosta et al. 2016), and average pore sizes were determined using the BJH model (Barrett et al. 1951) applied to the desorption branch of the isotherms. The pore size distributions of the ACs were determined by application of the non-linear density functional theory (NLDFT) (Jagiello & Olivier 2013) to the nitrogen adsorption branch. Secondary electrons were used for observing the topographic contrast of samples using scanning electron microscopy (FET Quanta 600 FEG), under an accelerating voltage of 3 kV.

In order to characterise the surface functional groups, infrared spectra of the powdered carbons were obtained with a Fourier-Transform Infrared (FTIR) spectrometer (PerkinElmer Spotlight Frontier) by doing 4 scans in the wavenumber range of 4000–650 cm^{-1} . The amount of proton-binding groups was also measured, and the total surface charge Q (mmol L^{-1}) was calculated. From these quantities, the numbers of groups having pK_a values in selected ranges could be calculated (Jagiello et al. 1995). For that purpose, 0.1 g of activated carbon was suspended in 50 mL of NaNO_3 solution (0.01 mol L^{-1}) as the supporting electrolyte and was stirred overnight to equilibrate. The suspension was then titrated with NaOH (0.1 mol L^{-1}) under N_2 saturation (Jagiello 1994) using an automatic titrator (905 Titrando, Metrohm commanded with tiamo® software V2.2).

2.3 Adsorption studies of Bisphenol A

BPA adsorption was thus investigated using the AC obtained showing the highest total surface area S_{TOT} , which was compared to that of the commercial AC (see subsection 3.2.2 below). Adsorption measurements were performed in hermetically closed glass vials, using 25 and 12.5 mg of TPC char and ACs, respectively, which were added to 25 mL of BPA solution. For the kinetic measurements at 25°C , initial BPA concentrations of 100 mg L^{-1} and 200 mg L^{-1} were used for TPC and ACs, respectively. The initial BPA concentrations used for building adsorption isotherms, i.e., at equilibrium, were ranging from 5 to 80 mg L^{-1} for TPC, and from 50 to 200 mg L^{-1} for ACs. Considering the low surface area of the TPC, we used twice as much the mass of AC and we lowered the BPA concentration in adsorption batches to avoid its fast saturation. BPA adsorption on TPC was done for the sole purpose of evaluating the

adsorption improvement after activation, although we are aware that a lower BPA concentration should decrease the equilibrium time.

The adsorbents in suspension in BPA solutions were magnetically stirred in a thermostatic water bath at 15, 25 or 35°C for building the equilibrium adsorption isotherms and doing the related thermodynamic analysis (see section 3.5). Initial pH values varied between 6.5 and 7.5, and were not adjusted for any tested material. After the adsorption equilibrium was reached, BPA concentration was measured with an UV/Vis spectrophotometer (Perkin Elmer Lambda 35) at a wavelength of 276 nm. To eliminate the effect of any contribution from soluble materials possibly released by the adsorbents, a blank was done. Particle attrition can indeed be a source of error when using UV spectroscopy. However, our experimental data were fitted extremely well by the selected models. We repeated several times some particular measurements, and the relative error was always lower than 2%.

The amount of BPA adsorbed by unit mass of sorbent, $q_{t,e}$, was calculated as:

$$q_{t,e} = \frac{V(C_0 - C_{t,e})}{m} \quad (1)$$

where C_0 and $C_{t,e}$ (mg L⁻¹) are the initial and equilibrium BPA concentrations, respectively, V (L) is the volume of solution and m (g) is the mass of sorbent. In order to account for the adsorption kinetics of BPA, the experimental data were fitted with pseudo-first and pseudo-second order kinetic models (Ho & McKay 1998; Ocampo-Pérez et al. 2012). The isotherm models listed in [Table 1](#) were used to fit the experimental adsorption data at equilibrium.

Isotherm	Nonlinear form	Parameters and units			Reference
Langmuir (<i>La</i>)	$q_e = \frac{q_{max} k_L C_e}{1 + k_L C_e}$	q_{max} [mg g ⁻¹]	k_L [L mg ⁻¹]		(Langmuir 1916)
Freundlich (<i>Fr</i>)	$q_e = k_F C_e^{1/n_f}$	k_F [mg g ⁻¹]	n_f^{-1}		(Freundlich 1907)
Sips (<i>Si</i>)	$q_e = \frac{q_{max} k_s C_e^{1/ns}}{1 + k_s C_e^{1/ns}}$	q_{max} [mg g ⁻¹]	k_s [L mg ⁻¹]	n_s^{-1}	(Sips 1950)
Dubinin-Radushkevich (<i>DR</i>)	$q_e = q_{max} \exp \left\{ - \left[\frac{RT \ln (C_s / C_e)}{E} \right]^2 \right\}$	q_{max} [mg g ⁻¹]	E [kJ mol ⁻¹]		(Dubinin & Radushkevich 1947)
Dubinin-Astokhov (<i>DA</i>)	$q_e = q_{max} \exp \left\{ - \left[\frac{RT \ln (C_s / C_e)}{E} \right]^n \right\}$	q_{max} [mg g ⁻¹]	E [kJ mol ⁻¹]	n	(Dubinin 1975)
Redlich – Peterson (<i>Re-Pe</i>)	$q_e = \frac{K_R C_e}{1 + a_R C_e^\beta}$	K_R [mg g ⁻¹]	a_R [L mg ⁻¹]	β	(Redlich & Peterson 1959)
Radke-Prausnitz (<i>Ra-Pr</i>)	$q_e = \frac{q_{mRP} K_{RP} C_e}{(1 + K_{RP} C_e)^{m_{RP}}}$	q_{mRP} [mg g ⁻¹]	K_{RP} [L mg ⁻¹]	m_{RP}	(Radke & Prausnitz 1972)

185

186 2.4 Thermodynamic study

187 The thermodynamic parameters: Gibbs free energy (ΔG°), enthalpy (ΔH°) and
 188 entropy (ΔS°), were calculated by the following equations.

$$189 \quad K_C = \frac{C_{Ad}}{C_e} \quad (2)$$

$$190 \quad \ln K_C = \frac{\Delta S^\circ}{R} - \frac{\Delta H^\circ}{RT} \quad (3)$$

$$191 \quad \Delta G^\circ = -RT \ln K_C \quad (4)$$

192 where K_C (dimensionless) is the equilibrium adsorption constant, which is the ratio of
 193 the residual equilibrium concentration of BPA in the solution, C_{Ad} (mg L⁻¹), to the

amount of BPA adsorbed onto the activated carbon at equilibrium, C_e (mg L⁻¹); T (K) is the temperature, and R (8.314 J mol⁻¹ K⁻¹) is the molar gas constant.

2.5 Regeneration and reuse study

CK.750.5 regeneration study was carried out as described elsewhere (Itodo and Oketunde, 2017). The first adsorption was carried out with 12.5 mg of CK.750.5 that were introduced in 25 mL of a 200 mg L⁻¹ BPA solution and stirred at 25°C for 24 h. The spent carbon was then separated and put in contact with 0.05 mL of a 0.1 mol L⁻¹ HCl aqueous solution and stirred for 24 h at 25°C. The solution was filtered, and the carbon was thoroughly washed with distilled water until neutral pH, and dried in an oven for 12 h at 85°C under vacuum. Finally, the regenerated carbon was submitted to BPA adsorption again, and the same adsorption-regeneration cycles were repeated 5 times.

3. Results and discussion

3.1 Pyrolysis process and products

Rubber tyre was pyrolysed in conditions presented in a previous publication (Acosta et al. 2015), and the detailed results were also given there. In summary, in the selected experimental conditions, 49.8 wt. % of oil, 40.1 wt. % of char and 10.1 wt. % of gas were obtained. The pyrolytic oil had a high heating value (HHV): 42.9 MJ kg⁻¹, on average, which is similar to that reported by some authors (Aylón et al. 2010; Quek & Balasubramanian 2013). The energy yield of this pyrolytic oil (HHV (MJ kg⁻¹) × oil yield (wt. %)) (Quek & Balasubramanian 2013) represents the amount of energy (in MJ)

that can be obtained per kg of scrap tyre used in the process. In the present case, the energy yield was obtained from the oil yield in the pyrolysis process and was found to be 22.7 % (MJ kg⁻¹).

This pyrolytic oil had an average density and viscosity of 0.949 g cm³ and 2.29 ×10⁻³ Pa s, respectively, similar to values already reported for other pyrolytic oils and close to those of commercial diesel fuel (Li et al. 2005). Finally, pyrolytic oil presented an acidity of 0.961 mg KOH g⁻¹ (a value representing the amount of KOH to neutralise 1 g of oil) above the permissible limit of 0.5 mg KOH g⁻¹ for being directly used as diesel fuel without oil upgrading, which is an essential but standard and cost-effective way to reduce its high acid content (Bacha et al. 2007). Tyre char composition was mainly 78.9 wt. % of fixed carbon, 6.9 wt. % of volatiles and 13.7 wt. % of ashes. The high carbon content of tyre char makes it a potentially good AC precursor.

3.2 Characteristics of tyre pyrolysis char and activated carbons

3.2.1 Elemental analysis

The ultimate compositions of TPC, CK.750.5 and CAC are presented in [Figure 2](#). In comparison, tyre scrap rubber contained 6% of ash and organic matter composed of 86 wt.% C (among which less than 30% is fixed carbon), 7.6 wt.% H, 3.2 wt.% O, 1.7 wt.% N and 1.6 wt.% S (Acosta et al. 2015).

After activation, the ash content increased in the TPC-derived material until 14.1 wt. %. Activation also induced a decrease of carbon content, while the oxygen content increased from around 3.3 to 7.8 wt. %, due to the formation of functional groups on the carbon surface. In a similar way, the sulphur content decreased with respect to TPC, which is attributed mainly to the volatility of this element. The same behaviour has been reported for ACs prepared under oxidising atmospheres (San Miguel et al. 2002).

Finally, the values of pH_{PZC} were 7.2 and 7.8 for TPC and CK.750.5, respectively, similar to those reported after chemical activation of scrap tyre rubber (Troca-Torrado et al. 2011). In contrast, the CAC had a pH_{PZC} of 10.7, which indicates possible activation in oxidising conditions (Bautista-Toledo et al. 2005).

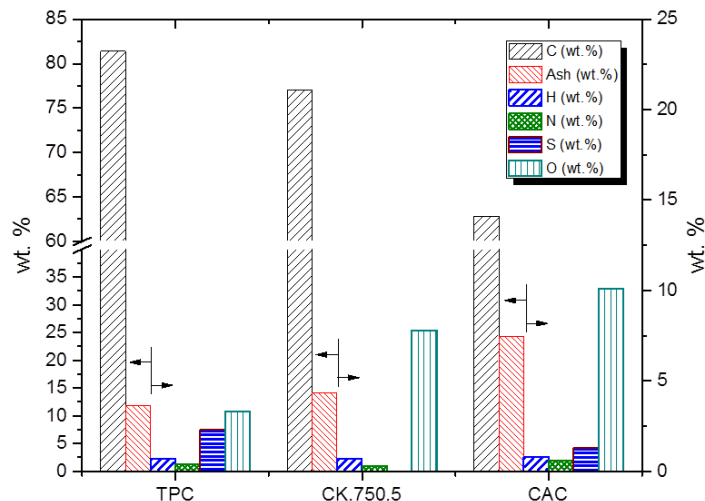


Figure 2. Ultimate analysis of tyre pyrolysis char and of the two activated carbons investigated here.

3.2.2 Surface area and porosity

After activation, the yield of sample CK.750.5 was 53 wt. %. The N_2 adsorption/desorption isotherms at -196°C of TPC, CK.750.5 and CAC are presented in **Figure 3(a)**. This figure presents the adsorption data with the X axis in logarithmic scale to better observe the pore volume filled at very low P/P_0 , from 10^{-7} , indicating the presence of very narrow pores in CK.750.5 and CAC. CK.750.5 and CAC exhibited isotherms of mixed Types I and IV, according to the IUPAC classification, and presented a linear part up to 150 and $100\text{ cm}^3\text{ g}^{-1}$, respectively, at relative pressures close to 0.01. TPC presented a predominantly Type IV isotherm according to the IUPAC classification, characteristic of mesoporous materials with a poorly developed microporous structure (San Miguel et al. 2001). The linear portion of those isotherms in

the range of medium P/P_0 (0.15-0.60) suggested multilayer adsorption in the mesopores. Only CAC showed a developed hysteresis loop (Type H4) within the range of relative pressures from 0.4 to 1, indicating the existence of a developed mesoporosity with slit-like mesopores. Type H4 loops are observed for many activated carbons and some other nanoporous adsorbents. (Sing & Williams 2004). CK.750.5 and TPC showed a sharp rise of the isotherms at P/P_0 close to 1, which is indicative of capillary condensation occurring in the meso- and macropores. Narrow hysteresis loops, Type H3, were observed for these two materials and therefore useful information can be obtained only by the application of the NLDFT method (Sing & Williams 2004). The pore-size distributions confirmed the presence of mesoporosity in CK.750.5 and TPC, with a maximum of porosity centred around 10 – 40 nm (Acosta et al. 2016).

Figure 3(b) presents the textural properties of TPC and ACs in terms of BET surface area, micropore and mesopore volumes. CK.750.5 exhibited a higher micro- and mesoporosity than CAC, and also a S_{BET} higher by $215 \text{ m}^2 \text{ g}^{-1}$. The CAC, Hydrodarco C, was supposed to present a surface area of $600 \text{ m}^2 \text{ g}^{-1}$, but the latter was found to be only $484 \text{ m}^2 \text{ g}^{-1}$. S_{BET} of CACs largely depends on the batch but also depends on the interval of relative pressures (P/P_0) used for applying the BET theory. We chose a range of P/P_0 ensuring that the C parameter was positive: we plotted $V_{ads} \times (1-P/P_0)$ as a function of P/P_0 , V_{ads} being the STP adsorbed volume, and took the range of P/P_0 values wherein $V_{ads} \times (1-P/P_0)$ increased with P/P_0 . Therefore, we totally trust the accuracy of our results. The microporous surface area of CK.750.5, determined by the t -plot method, was almost twice that of CAC, 414 and $210 \text{ m}^2 \text{ g}^{-1}$, respectively. The skeletal density was close to 2 for all materials (Acosta et al. 2016), while average pore sizes were 31.6, 18.3 and 6.7 nm, for TCP, CK.750.5 and CAC.

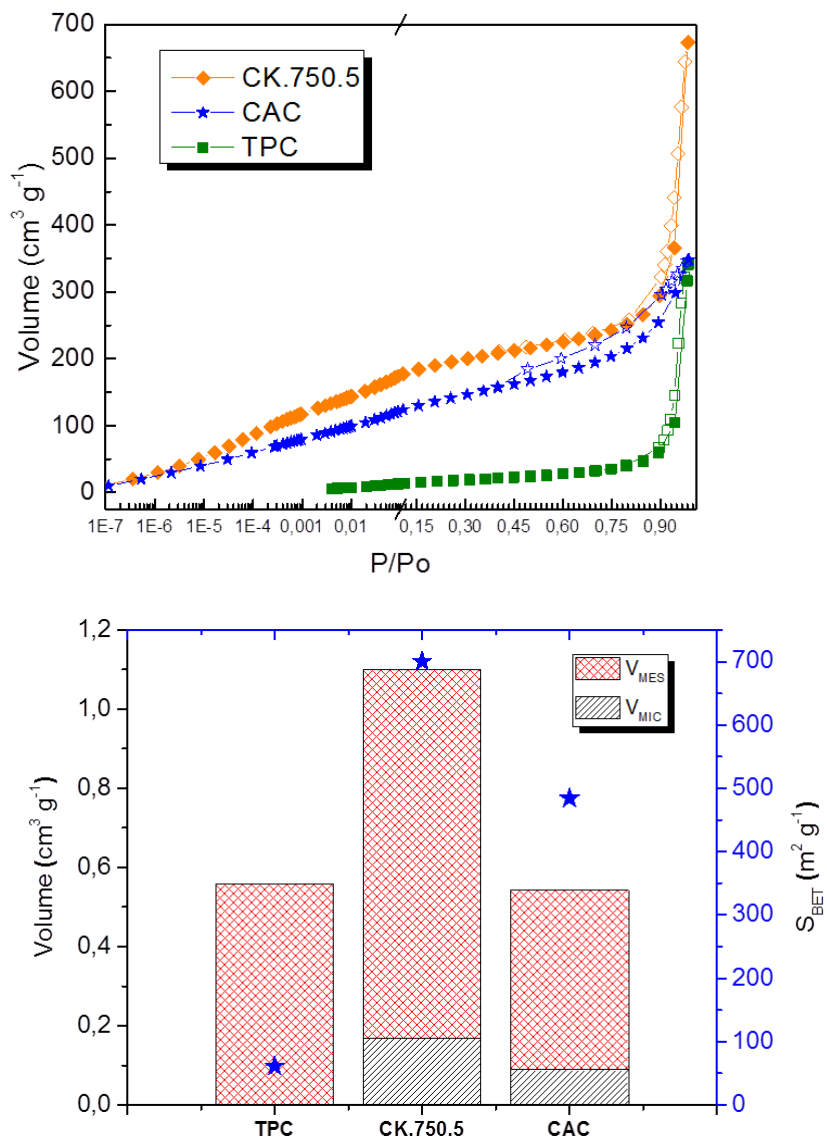


Figure 3. (a) N₂ adsorption/desorption isotherms of TPC, CK.750.5 and CAC at -196°C. For emphasising their differences in the range of low relative pressures, corresponding to microporosity, the scale of P/P₀ is logarithmic below 0.1 and linear above. (b) Textural characterisation of the same materials: V_{MIC} = micropore volume, V_{MES} = mesopore volume, and surface area (blue stars).

Figure 4 shows the results of the potentiometric titration for the three carbon materials studied therein. TPC had a total number of groups equal to 1.47 mmol g⁻¹ (as shown in Table 2), an amount far lower than what was determined for ACs: 3.37 and

3.99 mmol g⁻¹ for CAC and CK.750.5, respectively, in good agreement with the higher O and H contents observed by elemental analysis for ACs. The nature of the functional groups was also different. TPC had more basic (1.09 mmol g⁻¹) than acidic (0.38 mmol g⁻¹) groups.

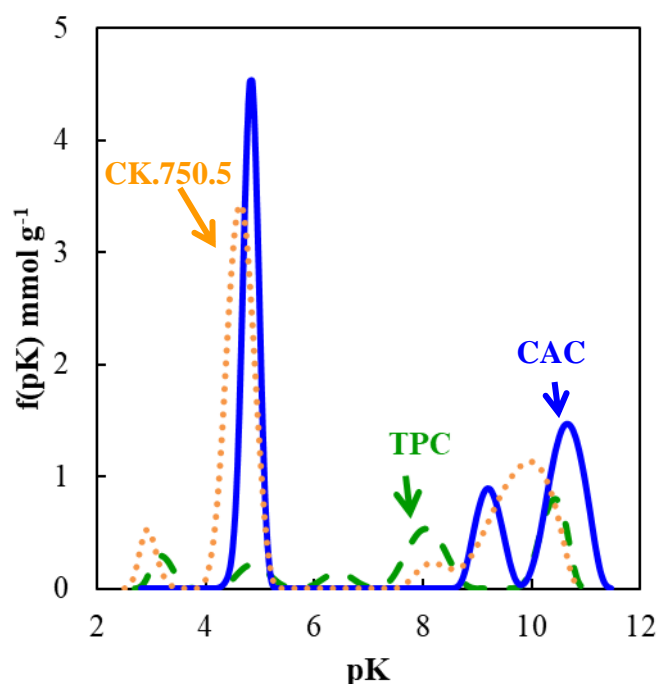


Figure 4. Density of functional groups as a function of pK_a , for TPC, CAC and CK.750.5

The pK_a distributions showed the predominance of strongly basic species such as lactol- or hydroxyl-containing functional groups with $pK_a > 8$ (Seredych et al. 2016). CAC presented almost balanced acidic and basic groups, and CK.750.5 had more acidic than basic groups. As it happened with TPC, strongly basic species, with $pK_a > 8$, were present in both ACs but acidic functions, with $pK_a < 5$, also existed. CAC and CK.750.5 presented 1.65 and 2.12 mmol g⁻¹ of acidic groups, which represent 49 and 53% of the total groups. The higher number of functional groups present in CK.750.5 might seem to disagree with the flatter IR profile shown in Figure S1 of the Supplementary

Information. However, FTIR spectroscopy may be quantitative as far as the corresponding data can be normalized with respect to the most intense band, which cannot be done here with so poorly characteristic spectra.

Table 2: Peak position and numbers of groups (in parentheses: (mmol g⁻¹)).

Sample	$pK_a < 3$	pK_a 3-5	pK_a 5-7	pK_a 7-8	pK_a 8-10	pK_a 10-12	acidic	basic	All
TPC	-	3.2 (0.14) 4.9 (0.15)	6.4 (0.09)	-	8.0 (0.15)	10.0 (0.46) 10.5 (0.48)	0.38	1.09	1.47
CK.750.5	2.9 (0.20)	4.6 (2.12)	-	-	8.2 (0.15)	10.0 (1.52)	2.12	1.67	3.99
CAC	-	4.82 (1.65)	-	-	9.2 (0.53)	10.6 (1.19)	1.65	1.72	3.37

From a practical and economic point of view, as important as the surface area is the material yield. The total surface area, S_{TOT} , was calculated by multiplying S_{BET} by the carbon yield. S_{TOT} was introduced elsewhere (Fierro et al. 2010) and can be used as a performance criterion for any process of porous carbon preparation. Several authors reported ACs prepared from tyre char having surface areas higher than ours (Mui et al. 2010b; Ariyadejwanich et al. 2003; González et al. 2006; San Miguel et al. 2003; Chan et al. 2011; Teng et al. 2000). However the total surface area (S_{TOT}) obtained in this study (371 m² g⁻¹), which represents the surface area obtained considering the mass loss during the activation process, is in the range of the results reported in the literature, and even higher in some cases, as indicated in Table 3. According to San Miguel et al. (San Miguel et al. 2001) the different surface areas that were reported may be attributed to differences in the activation and pyrolysis conditions, including furnace and tyre rubber characteristics.

Table 3. Main characteristics of tyre-derived ACs found in the literature and comparison with the present study.

References	Activating agent	S_{BET} ($\text{m}^2 \text{g}^{-1}$)	Yield (%)	S_{TOT} ($\text{m}^2 \text{g}^{-1}$)
This study	KOH	700	53	371
(Mui et al. 2010b)	CO ₂	1014	33	335
(Ariyadejwanich et al. 2003)	H ₂ O	1177	31.4	370
(González et al. 2006)	H ₂ O	1317	12.5	165
(San Miguel et al. 2003)	H ₂ O	1022	18	184
(Chan et al. 2011)	H ₂ O	962	15	144
(Teng et al. 2000)	KOH	474	-	-

3.3 Kinetics of BPA adsorption

Figure 5 a) shows the amount of BPA adsorbed per unit mass of adsorbent, q_t (mg g^{-1}), versus contact time, t (h), onto TPC, CK.750.5 and CAC. Equilibrium adsorption time was obtained after 4 h for TPC, and after 10 h for both CK.750.5 and CAC. Table 4 presents the corresponding experimental adsorption capacities at equilibrium for all materials. Figure 5 b) shows the BPA removal efficiency corresponding to the data of Figure 5 a). The BPA removal was around 7.5% for TPC, and around 15 and 20% for CAC and CK.750.5, respectively. Those modest BPA removals imply that higher ratios of sorbent to BPA solutions should be used to reach a more complete BPA elimination.

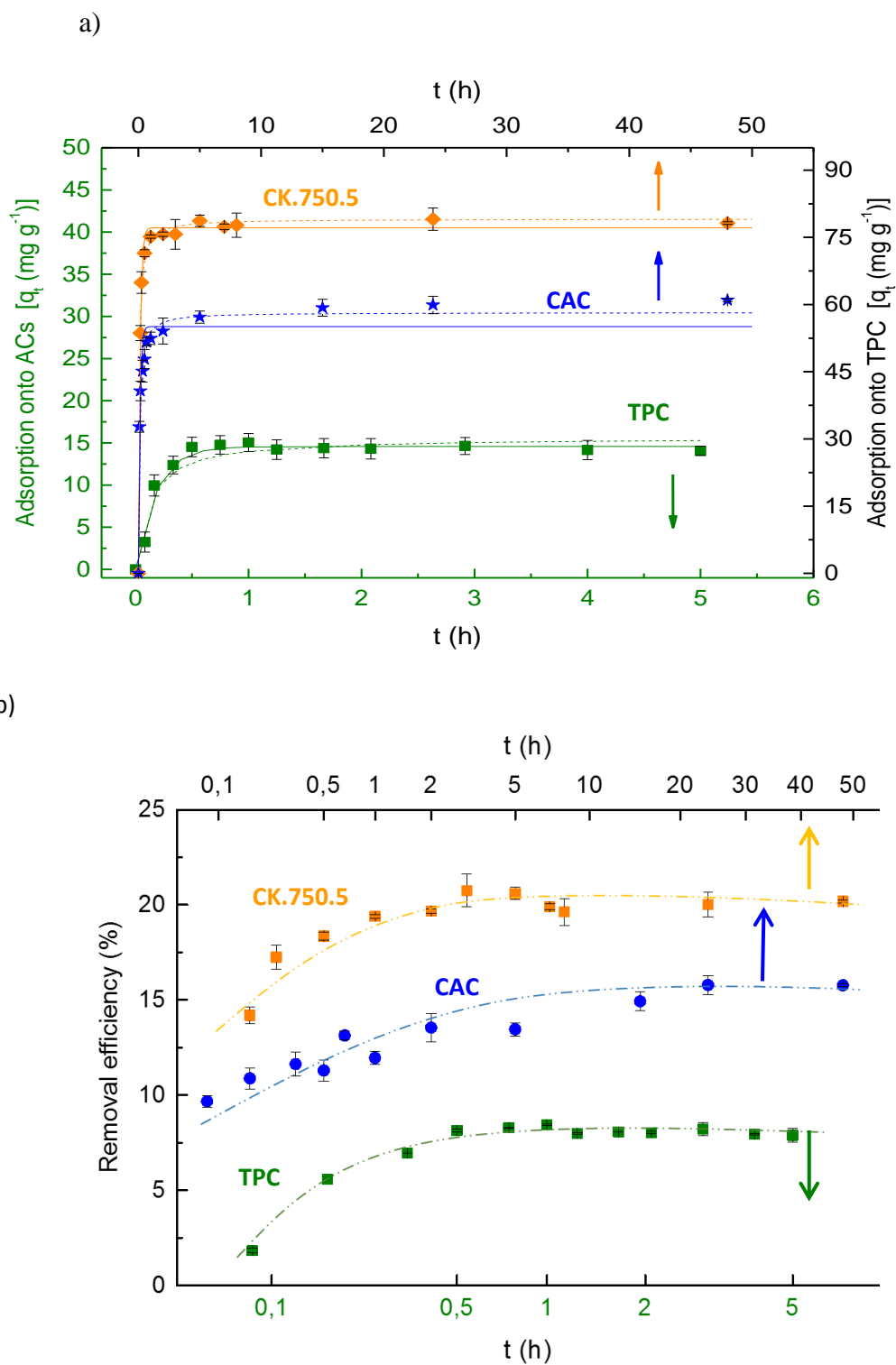


Figure 5. a) Adsorbed amounts of BPA at 25°C as a function of time, on TPC, CK.750.5 and CAC. Continuous and dotted lines represent the pseudo-first and pseudo-second order models, respectively. b) BPA removal at 25°C as a function of time, on TPC, CK.750.5 and CAC. Discontinuous lines are just guides for the eye. Experimental conditions were: $C_0 = 100 \text{ mg L}^{-1}$ and 200 mg L^{-1} for TPC and ACs, respectively; stirring speed 170 rpm, temperature 25°C, and pH 6.5 – 7.5. The data of TPC correspond to the top horizontal axis and the right vertical axis.

Table 4 also gathers the parameters derived from the fits of pseudo-first and pseudo-second order models to the experimental data, as well as the corresponding coefficients of determination, R^2 . The pseudo-second order model fitted the adsorption behaviour of ACs better, whereas the pseudo-first order model fitted that of TPC better. This suggests that adsorption of BPA onto TPC occurs mainly by a process of physical diffusion monolayer, while there is a rate-limiting step in the case of ACs, possibly chemical adsorption involving valence forces through exchange of electrons between sorbent and sorbate (Sulaymon et al. 2012). The adsorption capacities increased in the order $TPC < CAC < CK.750.5$ ($14.57 < 58.24 < 79.11 \text{ mg g}^{-1}$, respectively), indicating a faster saturation of TPC, mainly due to its lower S_{BET} .

Table 4. Adsorption rate constants, correlation coefficients and amounts of BPA adsorbed at equilibrium obtained by pseudo first- and pseudo second-order models.

	Pseudo-first order				Pseudo-second order		
	q_e (exp.) (mg g ⁻¹)	$k_l \times 10^{-2}$ (h ⁻¹)	R ²	q_e (predicted) (mg g ⁻¹)	$k_2 \times 10^{-4}$ (g (mg h) ⁻¹)	R ²	q_e (predicted) (mg g ⁻¹)
TPC	14.05	5.5	0.97	14.57	54.0	0.93	15.64
CK.750.5	78.19	7.1	0.99	77.17	19.0	0.99	79.11
CAC	60.99	8.3	0.93	55.09	22.0	0.99	58.24

3.4 BPA adsorption at equilibrium

3.4.1 General features of BPA adsorption isotherms

BPA adsorption capacity on TPC and ACs was calculated using Equation (1), and the adsorption isotherms were obtained at 25°C . The adsorption capacity, q_e (mg g^{-1}), was plotted versus the equilibrium concentration of the solute, C_e (mg L^{-1}), for TPC in Figure 6(a) and for both CK.750.5 and CAC in Figure 6(c). As it can be observed, the

increase of initial concentration leads to an increase of the BPA adsorption capacity,
which is due to a major saturation of the adsorbent surface.

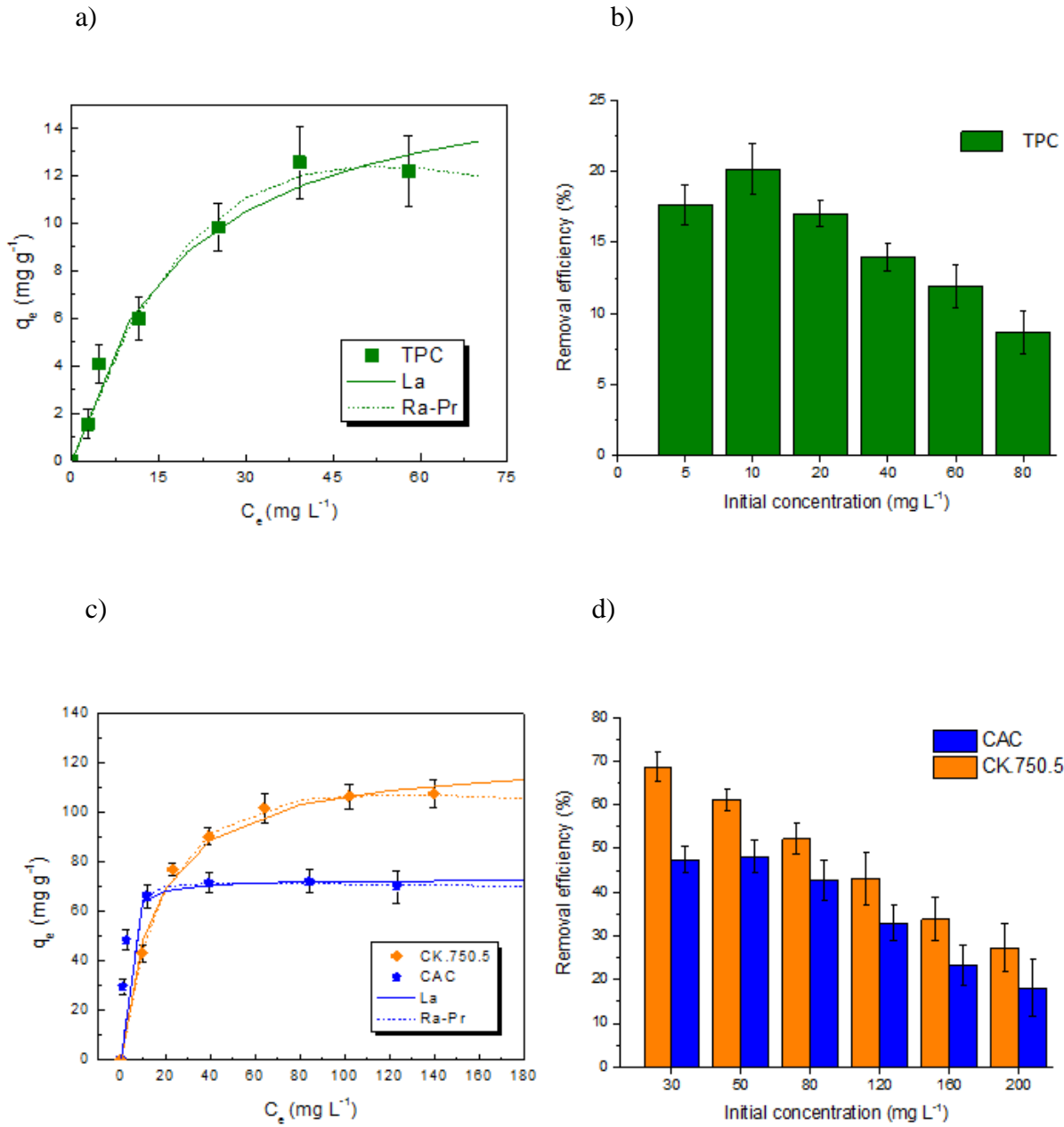


Figure 6. (a) BPA adsorption isotherm and b) BPA removal (%) on TPC. Experimental conditions were: $C_0 = 5 - 80$ mg L⁻¹, stirring speed 170 rpm for 8 h, temperature 25°C, and pH 6.5 – 7.5. (c) BPA adsorption isotherms and d) BPA removal (%) on CK.750.5 and CAC. Experimental conditions were: $C_0 = 30 - 200$ mg L⁻¹, stirring speed 170 rpm for 50 h, temperature 25°C, and pH 6.5 – 7.5. Continuous and dotted lines represent Langmuir (*La*) and Radke-Prausnitz (*Ra-Pr*) adsorption isotherm models, respectively.

Figure 6 also shows the BPA removal efficiency as a function of the initial concentration of BPA for TPC (b), and for CK.750.5 and CAC (d). Upon increasing the BPA initial concentration from 5 to 80 mg L⁻¹, the BPA removal efficiency on TPC decreased from around 20 to 10%. Using ACs instead, the BPA removal was considerably higher although it also decreased when the initial concentration of BPA increased, from around 70 to 30% for CK.750.5 and from around 50 to 20% for CAC. The parameters for the seven models presented in Table 1 and their corresponding determination coefficients are given in Table 5. In the case of Dubinin-Radushkevitch (*DR*) and Dubinin-Astakov (*DA*) adsorption isotherm equations, the saturation concentration, C_s , of BPA was 0.3 g L⁻¹ (Dehghani et al. 2016), which is the maximum BPA solubility in water at 25°C.

3.4.2 Discussion of BPA adsorption onto TPC and ACs

TPC was investigated separately due to its significantly different porosity with respect to ACs. The coefficient of determination, R^2 , presented in Table 5, gives the fitting of experimental data with respect to theoretical data. From the results obtained, it is clear that all models led to quite good fits ($R^2 > 0.97$), except the Freundlich model (0.94). According to the models comprising only two parameters, *La* and *DR*, the maximum adsorption capacities were 17.00 and 16.70 mg g⁻¹, respectively, while the maximum adsorption capacities obtained using *Si* and *DA* models were 15.53 and 14.54 mg g⁻¹, respectively. The energies of BPA adsorption onto TPC were 8.25 and 8.87 kJ mol⁻¹ according to *DR* and *DA* models, respectively. These values suggest a physisorption on the material, and similar results have indeed been obtained by applying the same models to materials such as chitosan (14.14 kJ mol⁻¹) (Dehghani et al. 2016) and BPA-imprinted microbeads (7.22 kJ mol⁻¹) (Bayramoglu et al. 2016).

The isotherm model parameters for CK.750.5 and CAC are also shown in Table 5. Most models allowed a good fit, with R^2 indeed higher than 0.96, except for the Freundlich (Fr) model ($R^2 = 0.79$). Langmuir (La) model led to one of the best fits, with which the maximum monolayer capacities were found to be 123.19 and 73.31 mg g^{-1} for CK.750.5 and CAC, respectively. These values are lower than those reported for commercial activated carbons having surface areas higher than $900 \text{ m}^2 \text{ g}^{-1}$ (Tsai et al. 2006).

Table 5. Isotherm model parameters obtained for the adsorption data of materials presented in this work at 25°C .

	Isotherm equation	Parameters						R^2
TPC	La	$q_{max} [\text{mg g}^{-1}]$	17.006	$k_L [\text{L mg}^{-1}]$	0.054			0.975
	Fr	$k_F [\text{mg g}^{-1}]$	1.813	n_f^{-1}	0.496			0.936
	Si	$q_{max} [\text{mg g}^{-1}]$	15.530	$k_s [\text{L mg}^{-1}]$	0.046	n_s^{-1}	1.132	0.976
	DR	$q_{max} [\text{mg g}^{-1}]$	16.688	$k [\text{kJ mol}^{-1}]$	8.252			0.971
	DA	$q_{max} [\text{mg g}^{-1}]$	14.540	$E [\text{kJ mol}^{-1}]$	8.875	n	2.614	0.976
	Re-Pe-	$k_R [\text{mg g}^{-1}]$	0.917	$a_R [\text{L mg}^{-1}]$	0.054	β	1.000	0.979
	Ra-Pr	$q_{mRP} [\text{mg g}^{-1}]$	149.520	$k_{RP} [\text{L mg}^{-1}]$	0.005	m_{RP}	4.946	0.982
CK.750.5	La	$q_{max} [\text{mg g}^{-1}]$	123.197	$k_L [\text{L mg}^{-1}]$	0.065			0.982
	Fr	$k_F [\text{mg g}^{-1}]$	30.836	n_f^{-1}	0.268			0.865
	Si	$q_{max} [\text{mg g}^{-1}]$	107.827	$k_s [\text{L mg}^{-1}]$	0.037	n_s^{-1}	1.296	0.964
	DR	$q_{max} [\text{mg g}^{-1}]$	117.355	$k [\text{kJ mol}^{-1}]$	9.138			0.962
	DA	$q_{max} [\text{mg g}^{-1}]$	108.527	$E [\text{kJ mol}^{-1}]$	8.684	n	3.286	0.999
	Re-Pe-	$k_R [\text{mg g}^{-1}]$	7.992	$a_R [\text{L mg}^{-1}]$	0.065	β	1.000	0.982
	Ra-Pr	$q_{mRP} [\text{mg g}^{-1}]$	205.743	$k_{RP} [\text{L mg}^{-1}]$	0.031	m_{RP}	1.266	0.996
CAC	La	$q_{max} [\text{mg g}^{-1}]$	73.310	$k_L [\text{L mg}^{-1}]$	0.677			0.990
	Fr	$k_F [\text{mg g}^{-1}]$	40.291	n_f^{-1}	0.134			0.787
	Si	$q_{max} [\text{mg g}^{-1}]$	71.754	$k_s [\text{L mg}^{-1}]$	0.610	n_s^{-1}	1.266	0.997
	DR	$q_{max} [\text{mg g}^{-1}]$	76.410	$k [\text{kJ mol}^{-1}]$	16.114			0.909
	DA	$q_{max} [\text{mg g}^{-1}]$	73.170	$E [\text{kJ mol}^{-1}]$	14.845	n	3.200	0.976
	Re-Pe-	$k_R [\text{mg g}^{-1}]$	49.609	$a_R [\text{L mg}^{-1}]$	0.677	β	1.000	0.990
	Ra-Pr	$q_{mRP} [\text{mg g}^{-1}]$	83.485	$k_{RP} [\text{L mg}^{-1}]$	0.532	m_{RP}	1.035	0.996

La isotherm refers to homogeneous adsorption and assumes the formation of a monolayer within which adsorption can only occur on a finite number of definite localised and equivalent sites (Foo & Hameed 2010), indicating that the different adsorption capacity of CK.750.5 with respect to CAC should be mainly attributed to a different surface area. K_L and K_F values for CAC were larger than for CK.750.5, indicating for CAC a higher affinity between adsorbate and adsorbent (Tsai et al. 2006). The mechanism proposed by Coughlin and Ezra (Coughlin & Ezra 1968) suggests that adsorption is based on π - π dispersion interactions between the electrons of the aromatic rings in the adsorbate and those of carbon basal planes in ACs. The protonation equilibria of BPA, which is a di-acid (see again Figure 1), were studied by a potentiometric method by Bautista-Toledo et al (Bautista-Toledo et al. 2005). The species distribution diagram showed that the first deprotonation of BPA starts at around pH 8.0 and the second one at around pH 9.0. The point of zero charge, pH_{PZC} , was very similar for TPC and CK.750.5 (7.2 and 7.8, respectively), while it was 10.7 for CAC. BPA adsorption was carried out at pH around 6.5 – 7.5, therefore BPA should be in its deprotonated form, while CK.750.5 and CAC should be positively charged, and CAC even more. Thus, the higher affinity of BPA for CAC cannot be explained by higher electrostatic interactions. CAC had higher heteroatom content than CK.750.5, essentially for oxygen and sulphur. Carbons containing more oxygen and sulphur are expected to be more hydrophilic, so the affinity for organic molecules such as BPA should be lower with CAC. However, CAC had a higher ash content that might explain the present results.

According to Foo and Hameed, (Foo & Hameed 2010), *Si* isotherm model is a combined form of *La* and *Fr* equations that was deduced for predicting heterogeneous adsorption. At low adsorbate concentrations, the behaviour is near that of *Fr* isotherm,

while at higher concentrations it predicts a monolayer adsorption characteristic of the *La* isotherm. In this work, the correlation coefficients of *Si* model were close to unity, allowing concluding that the maximal adsorption capacity of BPA of CK.750.5 and CAC are 108 and 72 mg g⁻¹, respectively, according to this model.

Using *DR* and *DA* models, it was possible to determine the mean free energy, which allows assigning, to a certain extent, the adsorption process to either a physical or a chemical mechanism. Thus, a value of free energy in the range of 5 – 40 kJ mol⁻¹ suggests a physical adsorption, while a value in the range of 40 – 800 kJ mol⁻¹ indicates a chemical adsorption (Liu et al. 2009). The free energy results obtained in this work for CK.750.5 and CAC were 9.1 and 16.1 kJ mol⁻¹ according to *DR*, respectively, and 8.7 and 14.8 kJ mol⁻¹ according to *DA*, respectively. Those values suggest that the adsorption of BPA onto ACs is a physisorption mechanism. Again, adsorption energies were higher for CAC, as predicted by the higher affinity found by application of *La* and *Fr* models.

Finally, *Re-Pe* and *Ra-Pr* models are hybrid isotherms featuring both *La* and *Fr* equations (Foo & Hameed 2010). For these models, the determination coefficients were the highest, i.e., close to one (see Table 5). The models have linear and power law dependences of concentration in the numerator and in the denominator, respectively. According to *Ra-Pr* equation, the calculated maximal adsorption capacities were always higher than those determined from the kinetic models and other isotherm models. Despite the good coefficients of determination (> 0.99), the maximum adsorption capacity determined by this model was very high and could not describe correctly the experimental equilibrium data. While in all cases the *Re-Pe* model reduced to the Langmuir equation ($\beta = 1$), and a_R was thus similar to the Langmuir adsorption constant (k_L).

Figure 7 shows the BPA adsorption capacities of the sorbents used in this work, as well as those reported in the open literature (Koduru et al. 2016; Bautista-Toledo et al. 2005; Tsai et al. 2006; Liu et al. 2009; Gong et al. 2016; Arampatzidou & Deliyanni 2016). A roughly linear correlation between S_{BET} and the maximum BPA adsorption capacity of the different ACs was observed. Discrepancies observed for a few data, seen to be out of trend, are most probably due to different moieties present at the surface of those ACs, as explained below for a few cases. However, this cannot be discussed much further due to the absence of information in most of the corresponding literature, or due to the use of different determination techniques preventing any straightforward comparison of adsorbents with each other. Moreover, our results showed the same trend with the surface area as those already presented by Arampatzidou and Deliyanni, (Arampatzidou & Deliyanni 2016), Tsai et al (Tsai et al. 2006) and Liu et al (Liu et al. 2009), dealing with ACs of higher surface area. Gong et al (Gong et al. 2016) obtained higher capacities than those reported here, due to the modification of the carbon surface through acidification with hydrochloric acid and subsequent functionalisation with addition of amino groups. Such a treatment can indeed shift the pH_{PZC} value and therefore may favour the adsorption of this type of compounds. On the contrary, Koduru et al (Koduru et al. 2016) and Bautista-Toledo et al (Bautista-Toledo et al. 2005) reported lower performances, possibly due to a lack of chemical interaction at the surface of the material, and due to the high pH_{PZC} value. In conclusion, tailoring the surface of the ACs for increasing electrostatic interactions between BPA and the sorbent is crucial to enhance the adsorption of BPA. Treatments such as acidification and functionalisation can improve the surface chemistry number of ACs, leading to higher interaction with the adsorbate. These assumptions are supported by the materials investigated here: coming back to Figure 3b) and to Table 2, the AC presenting the

highest BPA adsorption, CK.750.5, is the one both having the highest S_{BET} and bearing the highest number of acidic groups. The opposite is observed for TPC, exhibiting the lowest amount of acidic groups, the lowest surface area, and hence the lowest BPA uptake. CAC is in-between.

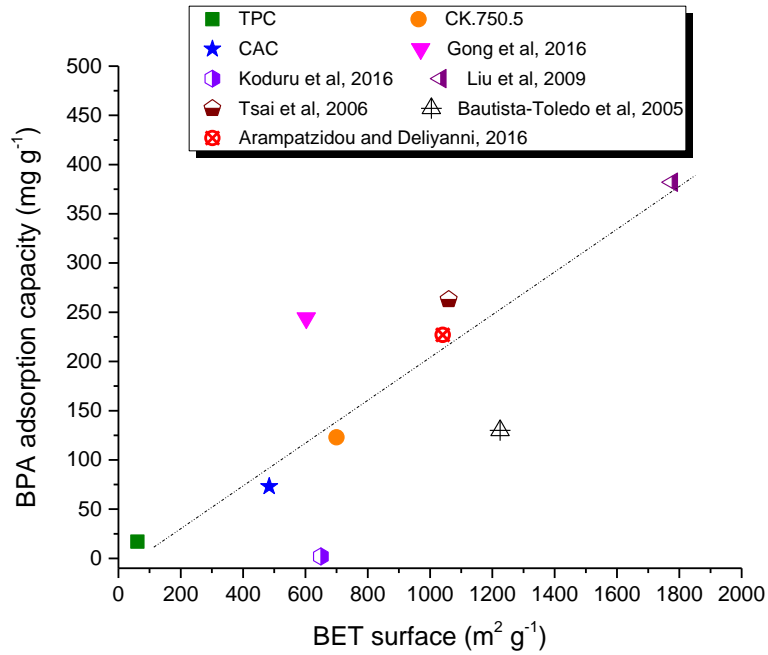


Figure 7. Literature review of BPA adsorption capacity of activated carbons produced in different conditions, as a function of their BET surface area. The straight line is just a guide for the eye.

3.5 Thermodynamic studies

The thermodynamic parameters of BPA adsorption onto CK.750.5 were evaluated by analysing the adsorption isotherms at different temperatures (15, 25 and 35°C), and using different initial concentrations. The results are gathered in Table 6.

Table 6. Thermodynamic parameters for BPA adsorption onto CK.750.5 calculated as a function of temperature and BPA initial concentration.

C_0 (mg L ⁻¹)	ΔH° (kJ mol ⁻¹)	ΔS° (J mol ⁻¹ K ⁻¹)	ΔG° (kJ mol ⁻¹)		
			15°C	25°C	35°C
31.52	-40.46	-128.76	-3.45	-2.09	-0.88
63.04	-16.11	-49.31	-1.95	-1.33	-0.97
86.68	-16.65	-53.41	-1.26	-0.73	-0.24
118.20	-10.53	-33.54	-1.22	-0.82	-0.20
157.60	-8.57	-27.43	-0.67	-0.42	-0.12
196.99	-8.71	-28.19	-0.67	-0.31	-0.12

These parameters indicate the sensitivity to temperature of BPA adsorption. BPA adsorption on CK.750.5 is an exothermic process, having a negative enthalpy (ΔH°) that produces a decrease in the adsorption capacity when the temperature increases. The absolute value of ΔH° increased considerably, from -8.71 to -40.46 kJ mol⁻¹, when the initial BPA concentration decreased from 197 to 31.5 mg L⁻¹. At low BPA concentrations, the most energetic sites are indeed occupied first and ΔH° indeed had a value close to what is considered to be the limit of chemical adsorption, but it steadily tended towards -10 kJ mol⁻¹, on average, at concentrations higher than 100 mg L⁻¹. These adsorption enthalpies are of the same order of magnitude as those reported in the literature for the adsorption on ACs of ceftazidime (19 kJ mol⁻¹) (Hu et al. 2017), dichromate (10 kJ mol⁻¹) (Maneechakr & Karnjanakom 2017), methylene green 5 (18 kJ mol⁻¹) (Tran et al. 2017) and mercury (25 kJ mol⁻¹) (Saleh et al. 2017).

The negative values obtained for the entropy (ΔS°) correspond to a decrease of disorder at the adsorbent–solution interface. Finally, the negative values for the Gibbs free energy (ΔG°) indicate that adsorption of BPA onto CK.750.5 is spontaneous and thermodynamically favourable in the limits of the experimental conditions used here. Moreover, when the temperature increased from 15 to 35°C, ΔG° decreased for all

initial concentrations employed, suggesting that adsorption is more spontaneous at lower temperature. The inversion temperature was calculated for all concentrations and varied from 41°C at 31.5 mg L⁻¹ to 36°C at 197 mg L⁻¹.

3.6 Regeneration and reuse study

Figure 8 shows the decrease of BPA adsorption performances of CK.750.5 after 5 consecutive cycles of regeneration and reuse. After the first adsorption-regeneration cycle, the BPA adsorption capacities decreased by 19%. Further adsorption-regeneration cycles had a lower effect as the adsorption capacity decreased by 5% at each new cycle, on average. Therefore, the initial BPA adsorption capacity was reduced by 41% after 5 adsorption-regeneration cycles. Such decrease might be due either to the irreversible adsorption of BPA on the sorbent that would limit further uptake, or to the modification of the surface functionalities related to washing with acid. BPA desorption might be improved by sonication in methanol or other organic solvents, as reported elsewhere (Sun & Weavers, 2006; Kwon et al, 2017).

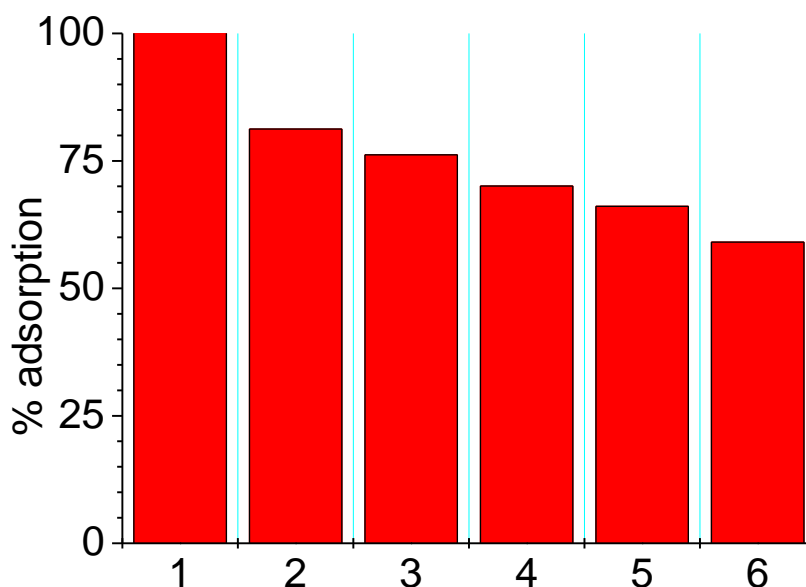


Figure 8. Changes of BPA adsorption after use and 5 additional regeneration-reuse cycles.

3.7 Economic considerations

About one billion units of scrap tyres per year are produced in the world, 200,000 units per year only in Colombia (Marin. 2012). Tyre manufacturing includes using different types of materials, such as natural rubber (NR) (22 -30 wt. %), synthetic rubber (styrene or butadiene rubber, SBR) (15 – 23 wt. %), carbon black (20 – 28 wt. %), steel (13 – 20 wt. %) and others (10 – 14 wt. %) (Sienkiewicz et al. 2012), depending on the future use of the tyre. The pyrolysis of rubber tyres leads to a range of valuable chemicals in solid (39 wt. %), liquid (53 wt. %) or gaseous form (8 wt. %), which can be used in petrochemical, energy or iron/steel industries after suitable processing. The pyrolysis gas is mainly composed of carbon dioxide, methane, hydrogen, ethane and ethylene, and the corresponding calorific values range from 29.9 to 42 MJ m⁻³, depending on the tyre brand (Kyari et al. 2005). These gases can be used to provide part of the energy requirements for the pyrolysis plant.

Otherwise, the calorific value of the tyre oil is approximately 43 MJ kg^{-1} , so the price of pyrolytic tyre oil could have similar a market value as the fuel oil, US\$ 45 per barrel (BP 2016) ($\approx \text{US\$ } 0.3 \text{ kg}^{-1}$). Economic viability is only obtained when pyrolysis processes are not limited to primary products but also induce higher value-added products: chemicals such as benzene, xylene and limonene, and/or high-quality carbon black and AC. For example, according to [Danon et al](#) (Danon et al. 2015), at least 2.5 wt. % of a steel-free tyre can be converted into dipentene (dl-limonene), which has a mean commercial value of $\text{US\$ } 2 \text{ kg}^{-1}$. 56 wt. % of activated carbon was obtained from pyrolytic char in this study; currently, the selling price of activated carbon from scrap tyre is set at $\text{US\$ } 2 \text{ kg}^{-1}$ (Alibaba 2016). CK.750.5, produced from tyres, has a moderate surface area and BPA adsorption capacity. However, it might be far cheaper than commercial ACs. From a practical point of view, one might indeed reasonably consider using twice as much activated carbon if it is four times cheaper. This choice would be rather dependent on adsorption reactors for existing industries, but it would not be limiting for new industries or rural communities. An ideal concept of pyrolytic tyre reprocessing into value-added products is presented in [Figure 9](#).

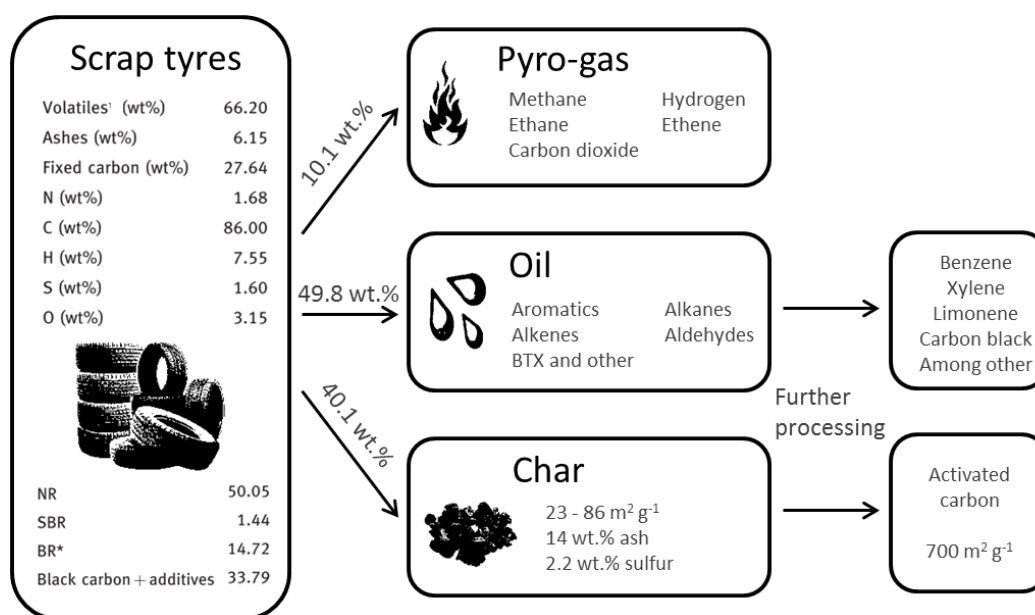


Figure 9. Summary of possible valorisation ways of waste tyres by pyrolysis.

According to the above, 100 kg of steel-free tyre would yield 22 kg of activated carbon, 50 kg of pyrolytic oil and 2.5 kg of limonene, taken as main value-added products. These products are estimated at about US\$ 44, US\$ 15 and US\$ 5, respectively, which mean an average appraisal of US\$ 6.4 per processed tyre, or US\$ 0.6 kg⁻¹, demonstrating the possibility of generating a profitable and environment-friendly environment process.

4. Conclusion

Activated carbons (ACs) with high BET surface area, 700 m² g⁻¹, can be produced from pyrolysis followed by chemical activation of scrap tyres and using KOH as activating agent. The as-obtained AC can be used as a potential adsorbent for the removal of pollutants such as Bisphenol A (BPA), showing a maximal BPA adsorption capacity of 123 mg g⁻¹, higher than the commercial activated carbon used as reference. Furthermore, the adsorption kinetics of BPA onto the investigated AC was well described by a pseudo-second order model. The isotherm adsorption parameters obtained from the fits of different models allowed determining the maximal adsorption capacity and describing the adsorption as a physical process, according to values of free energies. Finally, BPA adsorption onto tyre-derived AC was an exothermic process, i.e., favoured by the decrease of temperature. The utilisation of pyrolytic char as precursor of ACs would allow improving the economic balance of scrap tyres recycling to produce pyrolysis oils.

Supplementary information

FTIR spectra and SEM images are given as supplementary information.

627 Acknowledgments

628 D. Nabarlatz and R. Acosta acknowledge the Vicerectoría de Investigación y Extension
629 from the “Universidad Industrial de Santander” for financial support (Project 5457). R.
630 Acosta is grateful for the research grant “Young researcher 2012” of the Administrative
631 Department of Science, Technology and Innovation in Colombia COLCIENCIAS, to
632 the Physics-Chemistry Engineering Faculty and to the Chemical Engineering School
633 from the “Universidad Industrial de Santander” for the financial support during his
634 research internship.

References

- Acosta, R., Fierro, V., Martinez de Yuso, A., Nabarlantz, D. and Celzard, A. (2016) 'Tetracycline adsorption onto activated carbons produced by KOH activation of tyre pyrolysis char', *Chemosphere*, 149, pp. 168–176.
- Acosta, R., Tavera, C., Gauthier-Maradei, P. and Nabarlantz, D. (2015) 'Production of oil and char by intermediate pyrolysis of scrap tyres: Influence on yield and product characteristics', *International Journal of Chemical Reactor Engineering*, 13(2), pp. 189–200.
- Alamo-Nole, L. A., Perales-Perez, O. and Roman-Velazquez, F. R. (2011) 'Sorption study of toluene and xylene in aqueous solutions by recycled tires crumb rubber.', *Journal of hazardous material*, 185(1), pp. 107–11.
- Alibaba (2016) Activated carbon. Available at: <https://www.alibaba.com/showroom/tyre-activated-carbon-price.html>.
- Arampatzidou, A. C. and Deliyanni, E. A. (2016) 'Comparison of activation media and pyrolysis temperature for activated carbons development by pyrolysis of potato peels for effective adsorption of endocrine disruptor bisphenol-A', *Journal of Colloid and Interface Science*, 466, pp. 101–112.
- Ariyadejwanich, P., Tanthapanichakoon, W., Nakagawa, K. and Mukai, S. R. (2003) 'Preparation and characterization of mesoporous activated carbon from waste tires', *Carbon*, 41, pp. 157–164.
- Aylón, E., Fernández-Colino, A., Murillo, R., Navarro, M. V, García, T. and Mastral, A. M. (2010) 'Valorisation of waste tyre by pyrolysis in a moving bed reactor.', *Waste management*, 30(7), pp. 1220–4.
- Bacha, J., Freel, J., Gibbs, L., Hemighaus, G., Hoekman, K. and Horn, J. (2007) Diesel Fuels Technical Review, Chevron. Available at: http://www.chevronwithtechron.ca/products/documents/Diesel_Fuel_Tech_Review.pdf.
- Barrett, E. P., Joyner, L. G. and Halenda, P. P. (1951) 'The Determination of Pore Volume and Area Distributions in Porous Substances. I. Computations from Nitrogen Isotherms', *Journal of the American Chemical Society*, 73(1), pp. 373–380.
- Bautista-Toledo, I., Ferro-García, M. A., Rivera-Utrilla, J., Moreno-Castilla, C. and Vegas Fernández, F. J. (2005) 'Bisphenol A removal from water by activated carbon. Effects of carbon characteristics and solution chemistry.', *Environmental science & technology*, 39(16), pp. 6246–50.
- Bayramoglu, G., Arica, M. Y., Liman, G., Celikbicak, O. and Salih, B. (2016) 'Removal of bisphenol A from aqueous medium using molecularly surface imprinted microbeads', *Chemosphere*, 150, pp. 275–284.

BP (2016) BP Statistical Review of World Energy - Full report. Available at:
<http://www.bp.com/content/dam/bp/pdf/energy-economics/statistical-review-2016/bp-statistical-review-of-world-energy-2016-full-report.pdf>.

Carrott, P.J.M., Nabais, J.M.V, Carrott, M.M.L.R., Men, J.A. (2001) 'Thermal treatments of activated carbon fibres using a microwave furnace', *Microporous Mesoporous Mater.* 47, pp. 243–252.

Casajuana, N. and Lacorte, S. (2003) 'Presence and Release of Phthalic Esters and Other Endocrine Disrupting Compounds in Drinking Water', *Chromatographia*, 57, pp. 649-655.

Chan, O. S., Cheung, W. H. and McKay, G. (2011) 'Preparation and characterisation of demineralised tyre derived activated carbon', *Carbon*, 49(14), pp. 4674–4687.

Clara, M., Strenn, B., Saracevic, E. and Kreuzinger, N. (2004) 'Adsorption of bisphenol-A, 17 beta-estradiol and 17 alpha-ethinylestradiol to sewage sludge.', *Chemosphere*, 56(9), pp. 843–51.

Coughlin, R. W. and Ezra, F. S. (1968) 'Role of surface acidity in the adsorption of organic pollutants on the surface of carbon', *Environmental Science & Technology*, 2(4), pp. 291–297.

Dai, Y., Yao, J., Song, Y., Liu, X., Wang, S. and Yuan, Y. (2016) 'Enhanced performance of immobilized laccase in electrospun fibrous membranes by carbon nanotubes modification and its application for bisphenol A removal from water', *Journal of Hazardous Materials*, 317, pp. 485–493.

Danon, B., Van Der Gryp, P., Schwarz, C. E. and Görgens, J. F. (2015) 'A review of dipentene (dl-limonene) production from waste tire pyrolysis', *Journal of Analytical and Applied Pyrolysis*, 112, pp. 1–13.

Dehghani, M. H., Ghadermazi, M., Bhatnagar, A., Sadighara, P., Jahed-Khaniki, G., Heibati, B. and McKay, G. (2016) 'Adsorptive removal of endocrine disrupting bisphenol A from aqueous solution using chitosan', *Journal of Environmental Chemical Engineering*, 4(3), pp. 2647–2655.

Dubinin, M. M. (1975) *Physical Adsorption of Gases and Vapors in Micropores*, Progress in Surface and Membrane Science. ACADEMIC PRESS, INC.

Dubinin, M. M. and Radushkevich, L. V. (1947) 'The equation of the characteristic curve of the activated charcoal', *Proceedings of the USSR Academy of Sciences*, 50, pp. 331–337.

Fan, J., Yang, W. and Li, A. (2011) 'Adsorption of phenol, bisphenol A and nonylphenol ethoxylates onto hypercrosslinked and aminated adsorbents', *Reactive and Functional Polymers*, 71(10), pp. 994–1000.

Fierro, V., Muñiz, G., Basta, A. H., El-Saied, H. and Celzard, A. (2010) 'Rice straw as precursor of activated carbons: Activation with ortho-phosphoric acid', *Journal of Hazardous Materials*, 181(1–3), pp. 27–34.

709 Foo, K. Y. and Hameed, B. H. (2010) 'Insights into the modeling of adsorption isotherm
710 systems', *Chemical Engineering Journal*, 156(1), pp. 2–10.

711 Freundlich, H. (1907) 'Über die Adsorption in Lösungen', *Journal of Physical Chemistry*, 57(1).

712 Gong, Z., Li, S., Ma, J. and Zhang, X. (2016) 'Synthesis of recyclable powdered activated carbon
713 with temperature responsive polymer for bisphenol A removal', *Separation and*
714 *Purification Technology*, 157, pp. 131–140.

715 González, J. F., Encinar, J. M., González-García, C. M., Sabio, E., Ramiro, A., Canito, J. L. and
716 Gañán, J. (2006) 'Preparation of activated carbons from used tyres by gasification with
717 steam and carbon dioxide', *Applied Surface Science*, 252(17), pp. 5999–6004.

718 Gregg, S. J. and Sing, K. S. (1982) *Adsorption, Surface Area and Porosity*, Academic Press,
719 London.

720 Ho, Y. S. and McKay, G. (1998) 'Sorption of dye from aqueous solution by peat', *Chemical*
721 *Engineering Journal*, 70(2), pp. 115–124.

722 Hu, X., Zhang, H. and Sun, Z. (2017) 'Adsorption of low concentration ceftazidime from
723 aqueous solutions using impregnated activated carbon promoted by Iron, Copper and
724 Aluminum', *Applied Surface Science*, 392, pp. 332–341.

725 Itodo A.U. and Oketunde F.K. (2017) 'Activated Carbon: Spent, Regenerated and Reuse for
726 Synthetic Dyestuff Effluent Decolorization', *International Journal of Environmental*
727 *Monitoring and Protection*, 4(4), pp.29-37.

728 Jagiello, J. (1994) 'Stable Numerical Solution of the Adsorption Integral Equation Using Splines',
729 *Langmuir*, 10, pp. 2778-2785.

730 Jagiello, J., Bandosz, T.J., Putyera, K., Schwarz, J.A. (1995) 'Determination of Proton Affinity
731 Distributions for Chemical Systems in Aqueous Environments Using a Stable Numerical
732 Solution of the Adsorption Integral Equation', *Journal of Colloid and Interface Science*,
733 172 (2), pp. 341-346.

734 Jagiello, J., Ania, C., Parra, J.B., Cook, C. (2015) 'Dual gas analysis of microporous carbons using
735 2D-NLDFT heterogeneous surface model and combined adsorption data of N₂ and CO₂',
736 *Carbon*, 91, pp. 330-337.

737 Jagiello, J. and Olivier, J. P. (2013) '2D-NLDFT adsorption models for carbon slit-shaped pores
738 with surface energetical heterogeneity and geometrical corrugation', *Carbon*, 55, pp.
739 70–80.

740 Kan, Y., Yue, Q., Gao, B. and Li, Q. (2016) 'Comparison of activated carbons from epoxy resin of
741 waste printed circuit boards with KOH activation by conventional and microwave
742 heating methods', *Journal of the Taiwan Institute of Chemical Engineers*, 68, pp. 440–
743 445.

744 Koduru, J. R., Lingamdinne, L. P., Singh, J. and Choo, K.-H. (2016) 'Effective removal of
745 bisphenol A (BPA) from water using a goethite/activated carbon composite', *Process*
746 *Safety and Environmental Protection*. Institution of Chemical Engineers, 103, pp. 87–96.

747 Kwon, D.-S., Tak, S.-Y., Lee, J.-E., Kim, M.-K. Lee, Y.-H., Han, D.-W., Kang, S., Zoh, K.-D. (2017)
 748 'Desorption of micropollutant from spent carbon filters used for water purifier',
 749 Environmental Science and Pollution Research 24:17606–17615.

750 Kyari, M., Cunliffe, A. and Williams, P. T. (2005) 'Characterization of oils, gases, and char in
 751 relation to the pyrolysis of different brands of scrap automotive tires', Energy and Fuels,
 752 19(3), pp. 1165–1173.

753 Langmuir, I. (1916) 'The constitution and fundamental propperties of solids and liquids', in
 754 Journal of the American Chemical Society, pp. 2221–2295.

755 Li, S. Q., Yao, Q., Wen, S. E., Chi, Y. and Yan, J. H. (2005) 'Properties of pyrolytic chars and
 756 activated carbons derived from pilot-scale pyrolysis of used tires.', Journal of the Air &
 757 Waste Management Association (1995), 55(9), pp. 1315–26.

758 Lian, F., Song, Z., Liu, Z., Zhu, L. and Xing, B. (2013) 'Mechanistic understanding of tetracycline
 759 sorption on waste tire powder and its chars as affected by Cu(2+) and pH.',
 760 Environmental pollution, 178, pp. 264–70.

761 Liu, G., Ma, J., Li, X. and Qin, Q. (2009) 'Adsorption of bisphenol A from aqueous solution onto
 762 activated carbons with different modification treatments.', Journal of hazardous
 763 materials, 164(2–3), pp. 1275–80.

764 Manchón-Vizuet, E., Macías-García, A., Nadal Gisbert, A., Fernández-González, C. and Gómez-
 765 Serrano, V. (2005) 'Adsorption of mercury by carbonaceous adsorbents prepared from
 766 rubber of tyre wastes.', Journal of hazardous materials, 119(1–3), pp. 231–8.

767 Maneechakr, P. and Karnjanakom, S. (2017) 'Adsorption behaviour of Fe(II) and Cr(VI) on
 768 activated carbon: Surface chemistry, isotherm, kinetic and thermodynamic studies', The
 769 Journal of Chemical Thermodynamics, 106, pp. 104–112.

770 Marin., B. (2012) 'En favor del medio ambiente: de llanta de vieja a carbón activado.', Revista
 771 Universitas Científica, 15(1), pp. 32–35.

772 Mendoza-Carrasco, R., Cuerda-Correa, E. M., Alexandre-Franco, M. F., Fernández-González, C.
 773 and Gómez-Serrano, V. (2016) 'Preparation of high-quality activated carbon from
 774 polyethyleneterephthalate (PET) bottle waste. Its use in the removal of pollutants in
 775 aqueous solution', Journal of Environmental Management, 181, pp. 522–535.

776 Mita, L., Grumiro, L., Rossi, S., Bianco, C., Defez, R., Gallo, P., Mita, D. G. and Diano, N. (2015)
 777 'Bisphenol A removal by a Pseudomonas aeruginosa immobilized on granular activated
 778 carbon and operating in a fluidized bed reactor', Journal of Hazardous Materials, 291,
 779 pp. 129–135.

780 Mohapatra, D. P., Brar, S. K., Tyagi, R. D. and Surampalli, R. Y. (2011) 'Occurrence of bisphenol
 781 A in wastewater and wastewater sludge of CUQ treatment plant', Journal of Xenobiotics,
 782 1(1), pp. 9–16.

783 Mui, E. L., Cheung, W. H., Valix, M. and McKay, G. (2010a) 'Dye adsorption onto activated
784 carbons from tyre rubber waste using surface coverage analysis.', *Journal of colloid and*
785 *interface science*, 347(2), pp. 290–300.

786 Mui, E. L., Cheung, W. H., Valix, M. and McKay, G. (2010b) 'Mesoporous activated carbon from
787 waste tyre rubber for dye removal from effluents', *Microporous and Mesoporous*
788 *Materials*, 130(1–3), pp. 287–294.

789 Ocampo-Pérez, R., Rivera-Utrilla, J., Gómez-Pacheco, C. V, Sánchez-Polo, M. and López-
790 Peñalver, J. J. (2012) 'Kinetic study of tetracycline adsorption on sludge-derived
791 adsorbents in aqueous phase', *Chemical Engineering Journal*, 213, pp. 88–96.

792 Pachamuthu, M. P., Karthikeyan, S., Maheswari, R., Lee, A. F. and Ramanathan, A. (2017)
793 'Fenton-like degradation of Bisphenol A catalyzed by mesoporous Cu/TUD-1', *Applied*
794 *Surface Science*, 393, pp. 67–73.

795 Pan, B., Lin, D., Mashayekhi, H. and Xing, B. (2008) 'Adsorption and hysteresis of bisphenol A
796 and 17alpha-ethinyl estradiol on carbon nanomaterials.', *Environmental science &*
797 *technology*, 42(15), pp. 5480–5.

798 Quek, A. and Balasubramanian, R. (2013) 'Liquefaction of waste tires by pyrolysis for oil and
799 chemicals—A review', *Journal of Analytical and Applied Pyrolysis*, 101, pp. 1–16.

800 Radke, C. J. and Prausnitz, J. M. (1972) 'Adsorption of organic solutions from dilute aqueous
801 solution on activated carbon', *Industrial & Engineering Chemistry Fundamentals*, 11(4),
802 pp. 445–451.

803 Redlich, O. and Peterson, D. L. (1959) 'A Useful Adsorption Isotherm', *The Journal of Physical*
804 *Chemistry*, 63(6), pp. 1024–1026.

805 Rezg, R., El-Fazaa, S., Gharbi, N. and Mornagui, B. (2014) 'Bisphenol A and human chronic
806 diseases: Current evidences, possible mechanisms, and future perspectives.',
807 *Environment international*, 64, pp. 83–90.

808 Rochester, J. R. (2013) 'Bisphenol A and human health: A review of the literature',
809 *Reproductive Toxicology*, 42, pp. 132–155.

810 Saleh, T. A., Sari, A. and Tuzen, M. (2017) 'Optimization of parameters with experimental
811 design for the adsorption of mercury using polyethylenimine modified-activated
812 carbon', *Journal of Environmental Chemical Engineering*, 5(1), pp. 1079–1088.

813 San Miguel, G., Fowler, G. D., Dall'Orso, M. and Sollars, C. J. (2001) 'Porosity and surface
814 characteristics of activated carbons produced from waste tyre rubber', *Journal of*
815 *Chemical Technology & Biotechnology*, 77(1), pp. 1–8.

816 San Miguel, G., Fowler, G. D. and Sollars, C. J. (2002) 'The leaching of inorganic species from
817 activated carbons produced from waste tyre rubber.', *Water research*, 36(8), pp. 1939–
818 46.

819 San Miguel, G., Fowler, G. D. and Sollars, C. J. (2003) 'A study of the characteristics of activated
820 carbons produced by steam and carbon dioxide activation of waste tyre rubber', *Carbon*,
821 41(5), pp. 1009–1016.

822 Seredych, M., Biggs, M.J., Bandosz, T.J. (2016) 'Oxygen reduction on chemically heterogeneous
823 iron-containing nanoporous carbon: The effects of specific surface functionalities',
824 *Microporous Mesoporous Mater*, 221, pp. 137-149.

825 Sienkiewicz, M., Kucinska-Lipka, J., Janik, H. and Balas, A. (2012) 'Progress in used tyres
826 management in the European Union: A review.', *Waste management*, 32(10), pp. 1742–
827 51.

828 Sing, K. S. W. and Williams, R. T. (2004) 'Physisorption Hysteresis Loops and the
829 Characterization of Nanoporous Materials', *Adsorption Science & Technology*, 22(10),
830 pp. 773–782.

831 Sips, R. (1950) 'On the Structure of a Catalyst Surface. II', *The Journal of Chemical Physics*,
832 18(8), pp. 1024–1026.

833 Skodras, G., Diamantopoulou, I., Zabaniotou, A., Stavropoulos, G. and Sakellaropoulos, G. P.
834 (2007) 'Enhanced mercury adsorption in activated carbons from biomass materials and
835 waste tires', *Fuel Processing Technology*, 88(8), pp. 749–758.

836 Sulaymon, A. H., Mohammed, T. J. and Al-najar, J. (2012) 'Equilibrium and kinetics Studies of
837 Adsorption of Heavy Metals onto Activated Carbon', *Canadian Journal on Chemical*
838 *Engineering & Technology*, 3(4), pp. 86- 92.

839 Sun, P. and Weavers, L. K. 'Sonolytic reactions of phenanthrene in organic extraction
840 solutions', *Chemosphere*, Issue 11, 65 (11), pp. 2268-2274.

841 Sweetman, M.J., May, S. Mebberson, N., Pendleton, P, Vasilev, K., Plush, S.E., and Hayball, J.D.
842 (2017) 'Activated Carbon, Carbon Nanotubes and Graphene: Materials and Composites
843 for Advanced Water Purification', *Journal of carbon research*, 3 (18), pp. 1-29.

844 Teng, H., Lin, Y. and Hsu, L. (2000) 'Production of Activated Carbons from Pyrolysis of Waste
845 Tires Impregnated with Potassium Hydroxide', *Journal of the Air & Waste Management*,
846 50, pp. 1940–1946.

847 Tran, H. N., You, S.-J. and Chao, H.-P. (2017) 'Fast and efficient adsorption of methylene green
848 5 on activated carbon prepared from new chemical activation method', *Journal of*
849 *Environmental Management*, 188, pp. 322–336.

850 Troca-Torrado, C., Alexandre-Franco, M., Fernández-González, C., Alfaro-Domínguez, M. and
851 Gómez-Serrano, V. (2011) 'Development of adsorbents from used tire rubber', *Fuel*
852 *Processing Technology*, 92(2), pp. 206–212.

853 Tsai, W. T., Lai, C. W. and Su, T. Y. (2006) 'Adsorption of bisphenol-A from aqueous solution
854 onto minerals and carbon adsorbents.', *Journal of hazardous materials*, 134(1–3), pp.
855 169–75.

- 856 Vandenberg, L. N., Maffini, M. V., Sonnenschein, C., Rubin, B. S. and Soto, A. M. (2009)
857 'Bisphenol-a and the great divide: A review of controversies in the field of endocrine
858 disruption', *Endocrine Reviews*, 30(1), pp. 75–95.
- 859 Zhao, W., Fierro, V., Zlotea, C., Aylon, E., Izquierdo, M. T., Latroche, M. and Celzard, A. (2011)
860 'Optimization of activated carbons for hydrogen storage', *International Journal of*
861 *Hydrogen Energy*, 36(18), pp. 11746–11751.
- 862 Zhu, H. and Li, W. (2013) 'Bisphenol A removal from synthetic municipal wastewater by a
863 bioreactor coupled with either a forward osmotic membrane or a microfiltration
864 membrane unit', *Frontiers of Environmental Science and Engineering*, 7(2), pp. 294–300.

865

Figure captions

Figure 1. Molecular structure of Bisphenol A (BPA).

Figure 2. Ultimate analysis of tyre pyrolysis char and of the two activated carbons investigated here.

Figure 3. (a) N₂ adsorption/desorption isotherms of TPC, CK.750.5 and CAC at -196°C. For emphasising their differences in the range of low relative pressures, corresponding to microporosity, the scale of P/P_0 is logarithmic below 0.1 and linear above. (b) Textural characterisation of the same materials: V_{MIC} = micropore volume, V_{MES} = mesopore volume, and surface area (blue stars).

Figure 4. Density of functional groups as a function of pK_a , for TPC, CAC and CK.750.5

Figure 5. a) Adsorbed amounts of BPA at 25°C as a function of time, on TPC, CK.750.5 and CAC. Continuous and dotted lines represent the pseudo-first and pseudo-second order models, respectively. b) BPA removal at 25°C as a function of time, on TPC, CK.750.5 and CAC. Discontinuous lines are just guides for the eye. Experimental conditions were: $C_0 = 100 \text{ mg L}^{-1}$ and 200 mg L^{-1} for TPC and ACs, respectively; stirring speed 170 rpm, temperature 25°C, and pH 6.5 – 7.5. The data of TPC correspond to the top horizontal axis and the right vertical axis.

Figure 6. (a) BPA adsorption isotherm and b) BPA removal (%) on TPC. Experimental conditions were: $C_0 = 5 - 80 \text{ mg L}^{-1}$, stirring speed 170 rpm for 8 h, temperature 25°C, and pH 6.5 – 7.5. (c) BPA adsorption isotherms and d) BPA removal (%) on CK.750.5 and CAC. Experimental conditions were: $C_0 = 30 - 200 \text{ mg L}^{-1}$, stirring speed 170 rpm for 50 h, temperature 25°C, and pH 6.5 – 7.5. Continuous and dotted lines represent Langmuir (La) and Radke-Prausnitz ($Ra-Pr$) adsorption isotherm models, respectively.

Figure 7. Literature review of BPA adsorption capacity of activated carbons produced in different conditions, as a function of their BET surface area. The straight line is just a guide for the eye.

Figure 8. Changes of BPA adsorption after use and 5 additional regeneration-reuse cycles.

Figure 9. Summary of possible valorisation ways of waste tyres by pyrolysis.